



# Design and Development of an Adaptive Robotic Gripper

Sainul Islam Ansary<sup>1</sup> · Sankha Deb<sup>2</sup> · Alok Kanti Deb<sup>3</sup>

Received: 9 September 2022 / Accepted: 9 August 2023 / Published online: 31 August 2023  
© The Author(s), under exclusive licence to Springer Nature B.V. 2023

## Abstract

In this paper, the design and development of an adaptive gripper are presented. Adaptive grippers are useful for grasping objects of varied geometric shapes by wrapping fingers around the object. The finger closing sequence in adaptive grippers may lead to ejection of the object from the gripper due to any unbalanced grasping force and such grasp failure is common for lightweight objects. Designing of the proposed gripper is focused on ensuring a stable grasp on a wide variety of objects, especially, lightweight objects (e.g., empty plastic bottles). The proposed actuation mechanism is based on movable pulleys and tendon wires which ensure that once a link stops moving, the other links continue to move and wrap around the object. Further, optimisation is used to improve the design of the adaptive gripper and the optimised gripper has been developed using 3D printing. Finally, validation is done by executing object grasping on common household objects using an industrial robot fitted with the developed gripper.

**Keywords** Robot hands/grippers · Tendon-driven mechanisms · Underactuation · Stable grasp

## 1 Introduction

In a robotic system for object handling, robot grippers play a crucial role to support the grasping and manipulation of objects of diverse geometric shapes. Most of the mechanical grippers used in industrial robots for handling objects are simple two-finger parallel grippers, which are custom engineered for grasping objects of a particular geometric shape like cuboidal, cylindrical, spherical, etc. However, they lack the grasping flexibility to adapt to objects of varied geometric shapes as encountered during object handling operations and are found unsuitable for performing different types of grasps (e.g., enveloping, fingertip, etc.) depending upon the

object geometry. On the other hand, service robots use dexterous multi-finger hands/grippers for performing more complex grasping and manipulation tasks. However, the design of a multi-finger anthropomorphic hand is very challenging. That is one of the main reasons for applications of these multi-finger grippers to remain in the research domain [1].

A major challenge for robot gripper design is the limited physical space available within the fingers. One way to overcome the problem could be the utilisation of various underactuated mechanisms. Underactuation reduces the complexity of the finger actuation system and requires a lesser number of actuators than the total degrees of freedom, thus making the gripper smaller and more lightweight. It is desirable for such mechanisms to be shape-adaptive (i.e., the gripper wraps/envelops its fingers around the irregularly shaped object) and the grasping force should be well distributed around the object for maintaining a stable grasp. In the past, different variations of differential mechanisms have been used to design such adaptive grippers [2], e.g., movable pulley [3], planetary or bevel gear differentials [4], seesaw mechanisms such as differential lever [5], equalizing bar [6], lockable differential mechanism [7], etc. Other than the differential mechanisms, based on the requirements, underactuated mechanisms can also be realised using linkages, tendon wires, gear trains [8], belts and pulleys [9], timing belts [10], flexible drive trains [11] and so on. A number of robotic hands/grippers based on underactuated mechanisms

Sainul Islam Ansary  
sainul@iitkgp.ac.in

Sankha Deb  
sankha.deb@mech.iitkgp.ac.in

Alok Kanti Deb  
alokkanti@ee.iitkgp.ac.in

<sup>1</sup> Advanced Technology Development Centre, IIT Kharagpur,  
721302 Kharagpur, India

<sup>2</sup> Mechanical Engineering Department, IIT Kharagpur,  
721302 Kharagpur, India

<sup>3</sup> Electrical Engineering Department, IIT Kharagpur,  
721302 Kharagpur, India

by means of linkages and tendon-pulley networks can be found in the literature [12]. The linkage mechanism consists of rigid bars connecting the finger phalanges to the actuator at the base joint. Most of the linkage driven mechanisms use four-bar linkages, but more than four numbers of linkages have also been used for realising complex spatial mechanisms. Detailed literature on the different design configurations of four-bar linkage mechanisms for robotic finger actuation can be found in [13]. The underactuated four-bar linkage uses passive elastic elements to make the mechanism shape-adaptive for example, extension springs in [14], pre-tightening torsional springs in [15], spring loaded sliding blocks in [16], compression springs in [17], and spiral springs in [18].

Inspired by the tendon networks in the human body, the use of tendons can be found in different robotic grippers. One of the earliest works on the tendon-driven mechanism was proposed and designed by Hirose and Umetani [19], commonly known as a soft gripper. The simple and lightweight soft gripper mechanism inspired a number of other designs. For example, the design of the high-speed capturing robot gripper [20] and the prosthetic hand [21] were based on the soft gripper mechanism. The Barrett hand is a commercially available three-finger underactuated gripper. The gripper uses a novel breakaway transmission mechanism [9] for realising the adaptive/ enveloping grasp. In [22], a self-adaptive mechanism based on cable transmission and compression springs was designed. A highly underactuated anthropomorphic robotic hand using a differential mechanism based on tendon-pulley was presented in [23]. The Velo gripper [24] is a two-finger adaptive gripper based on active tendons and spring loaded passive tendons claimed to be effective at performing enveloping and parallel/fingertip grasps. An underactuated three-finger gripper using only a single tendon and spiral springs for each finger was proposed in [25].

As evident from the above literature review, a variety of mechanisms had been previously employed for transmitting power to the joints, such as tendons, linkages, gear trains, belts and pulleys, timing belts, flexible drive trains and so on. However, each mechanism has its own set of drawbacks, e.g. high friction in tendons, design complexity and bulkiness in linkages, backlash and vibration in gears, slacking in belts, etc. The choice of a specific design method out of the many design concepts and options purely depends on the field of application and its requirements. Tendon Driven Mechanism (TDM) offers advantages over other actuation mechanisms, especially in terms of compact design and lightweight. In addition, the combination of tendons and springs exhibits inherent compliance, which is a requirement for a system interacting with the environment. However, such a mechanism encounters problems when handling lightweight objects (e.g., empty plastic bottles) during envelope/

power grasp, which may lead to ejection of the object from the gripper due to any unbalanced grasping force. Keeping the limitations in mind, it is, therefore, necessary to develop simple actuation mechanisms putting more emphasis on grasp stability. The main focus of the current work is on the design aspects to solve the problem of object ejection, especially for lightweight objects during the envelope/power type of grasps. Although the TDM offers various advantages, it also add complexities in terms of control aspects [26], where various uncertainties [27], modelling errors, and disturbance/noise need to be handled for robust control. The controller design is out of the scope for the current work, but will be considered for the future work.

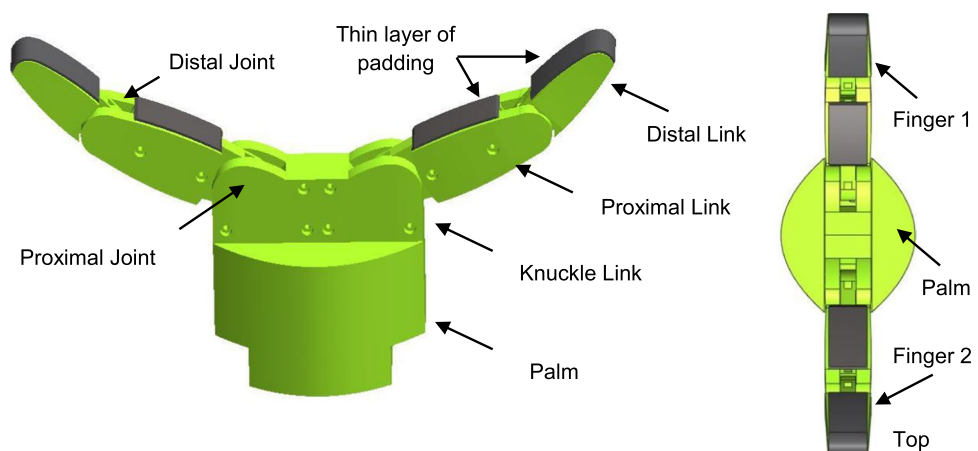
In this work, keeping the above in mind, tendon driven mechanism is preferred over other mechanisms (e.g., linkages, gear train etc.) to achieve the desired finger motion. A simple underactuation actuation mechanism based on a movable pulley and tendons is proposed with the goal of ensuring simultaneous closing of the finger links. Then, a two-finger gripper based on the proposed actuation mechanism is designed which is capable of dealing with lightweight objects and performing the adaptive type of grasp on irregularly shaped objects. Further, a framework for optimisation of the gripper design and actuation mechanism is presented. Then, the optimised gripper is fabricated using 3D printing technology. Further, integration of actuators and position sensors to the gripper is also given. Finally, the developed gripper is integrated with an industrial robot and experimental results of grasping common objects are demonstrated.

The rest of the paper is organized as follows. Section 2 presents the proposed actuation mechanism, design of the adaptive gripper, the optimisation framework, integration of actuators and sensors, and fabrication of the gripper. Section 3 demonstrates the experimental results. Finally, Sect. 4 gives the conclusion.

## 2 Design of the Proposed Gripper

This work is mainly focused on designing a simple adaptive gripper, which can perform both enveloping/power and fingertip/precision types of grasps. A model of the proposed two-finger robotic gripper is shown in Fig. 1. The gripper consists of two identical fingers, each having three links namely, knuckle, proximal and distal, and a palm. Knuckles are fixed on the palm and give support to an object during the enveloping/wrapping type of grasp. The knuckle-proximal and proximal-distal links are connected using two revolute joints to form an articulated finger. Both joints of each finger are actuated by only one DC motor. The motors are embedded inside the palm. A proposed tendon-spring system as given the next section is used to achieve the flexion and extension motion of the middle and distal links in each

**Fig. 1** Model of the two-finger adaptive robotic gripper



finger. A thin layer of padding is provided on the contact areas of each finger to distribute grasping force over a larger contact surface which helps to stabilise the object grasping. The kinematics of the gripper is given in appendix-A.

## 2.1 Design of the Proposed Tendon-Driven Actuation Mechanism

Adaptive underactuated grippers adapt the shape of an object by wrapping the fingers around the object and usually have a lesser number of actuators than the total number of degrees of freedom (dofs). The underactuated mechanism reduces the number of actuators which makes the design small, lightweight, and simple while keeping the gripper capability to adapt an object shape. A class of underactuated mechanisms [21, 22, 25, 28] are designed in such a way that the first link starts to move when actuation force is applied and the subsequent links only move once the precedent link touches an object or maximum joint limit reached as shown in Fig. 2(a). Such a mechanism encounters problems when handling lightweight objects (e.g., empty plastic bottles) during envelope/power grasp. Once the first link of each gripper finger makes contact with the object, the resulting contact force pushes the object outward away from the gripper and breaks the contacts. Then the first link moves further to make contact with the object at a different location and the contact force further pushes the object outward. Meanwhile, the subsequent links do not move as the first link could not make

stable contact and the object eventually slips away from the gripper as shown in Fig. 2(b).

A solution to the object slipping away from the gripper can be simultaneously closing all the links and once a preceding link makes contact with the object or the maximum limit is reached, the subsequent links continue to move. To achieve the desired finger motion, the actuation force is transmitted from an actuator to the finger links through tendon wires. The tendon mechanism needs to distribute the actuation force to the links in such a fashion that the links start to move simultaneously and once a link touches an object or the maximum joint limit is reached, the subsequent links continue to move.

In order to make the mechanism work, a network of bifurcated tendons originating from the actuator and comprising of a combination of stretchable and non-stretchable tendon elements can be used with certain advantages and disadvantages. A generalisation of the network with only non-stretchable tendons for  $n$  number of joints is shown in Fig. 3(a). The basic design of the network is that a single tendon originating from an actuator bifurcates into two branches at each joint of a finger. One branch is fixed with the immediate link of the joint and the other branch runs through the link, only to bifurcate at the next joint of the articulated finger.

Let  $n$  be the number of joints,  $d_l^1$  and  $d_l^2$  be the instantaneous tendon displacements of the two branches at  $j$ -th joint,  $d_{q_j}$  be the instantaneous joint displacements of  $j$ -th joint. For non-stretchable tendons, the displacements are equal for the tendon branches

**Fig. 2** (a) a joint starts to move only after the preceding link touching an object resulting in an enveloping grasp, (b) The closing of the fingers moves the object causing it to slip away from the finger

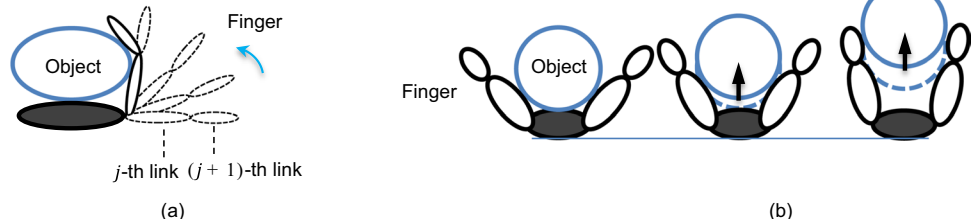
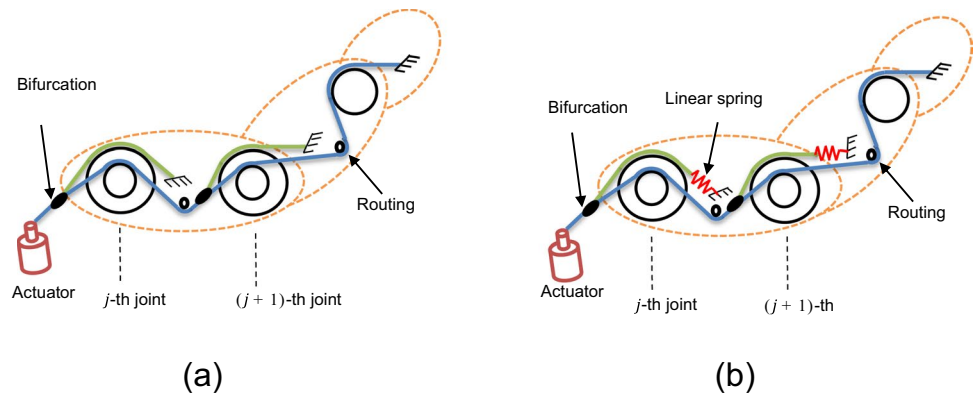


**Fig. 3** (a) Tendon network with non-stretchable tendons, (b) Tendon network with spring loaded stretchable tendons



$$dl_j^1 = dl_j^2 \quad (1)$$

For the  $j$ -th and  $(j+1)$ -th joints, the relation between the tendon displacement and the joint displacements is as follows.

$$dl_j^1 = r_j^1 dq_j \quad (2)$$

$$dl_j^2 = r_j^2 dq_j + r_{j+1}^1 dq_{j+1} \quad (3)$$

The Eqs. 2 and 3 give the coupling relation between the joints as follows.

$$dq_{j+1} = \frac{(r_j^1 - r_j^2)}{r_{j+1}^1} dq_j \quad (4)$$

where,  $r_j^1$  and  $r_j^2$  are the pulley radii of the two tendon branches at  $j$ -th joint.

Now, when  $j$ -th link stops once it touches an object or the maximum limit is reached, i.e.  $q_j = 0$ , from Eq. 4 the  $(j+1)$ -th link also stops, which implies that the mechanism is underactuated but not adaptive. To make the mechanism adaptive, a stretchable tendon element is introduced in the first branch as shown in Fig. 3(b). A linear spring at the end of the tendon can be added to make the tendon stretchable [29]. The relation between the tendon displacement and the joint displacements given in Eq. 2 is modified for the stretchable spring-loaded tendon as follows.

$$dl_j^1 = \delta l_j^1 + r_j^1 dq_j \quad (5)$$

where,  $\delta l_j^1$  is the elongation of the stretchable tendon. Then, Eqs. 3 and 5 give

$$dq_{j+1} = \frac{1}{r_{j+1}^1} \delta l_j^1 + \frac{(r_j^1 - r_j^2)}{r_{j+1}^1} dq_j \quad (6)$$

So, once a link stops, the subsequent link continues to move depending on the elongation of the stretchable tendon.

Let  $f_j^1$  and  $f_j^2$  be the tendon forces of the two branches at the  $j$ -th joint,  $\tau_j$  be the joint torque at the  $j$ -th joint. Now, the actuation force is equally divided at each bifurcation and the actuation torque generated by tendon branches depends on the moment arm of the associated joint pulley for each branch. Then, the tendon force at  $j$ -th bifurcation as well as the relation between the tendon force and joint torque are as follows.

$$f_j^1 = f_j^2 = f/2^j \quad (7)$$

$$\tau_j = r_j^1 f_j^1 + r_j^2 f_j^2 \quad (8)$$

where  $f$  is the force generated by the actuator.

Although the use of a linear spring makes the design simple, the selection of the linear spring constant of the stretchable tendon is challenging. Here, an alternative mechanism is proposed to make the gripper adaptive and it works similar to the mechanism having stretchable tendons. The tendon network of the proposed mechanism consists of non-stretchable tendons and movable pulley mechanisms which are used for the tendon bifurcation as shown in Fig. 4. The non-stretchable tendon

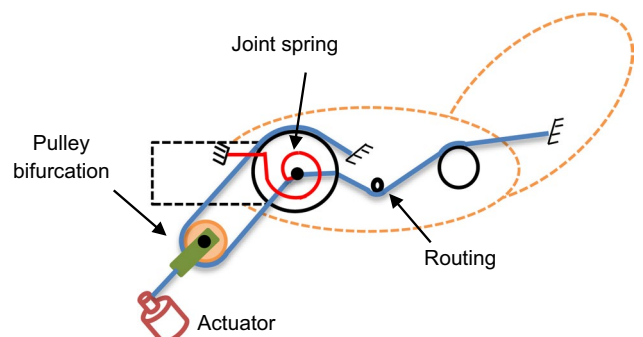


**Fig. 4** Tendon network with pulley mechanism and non-stretchable tendons

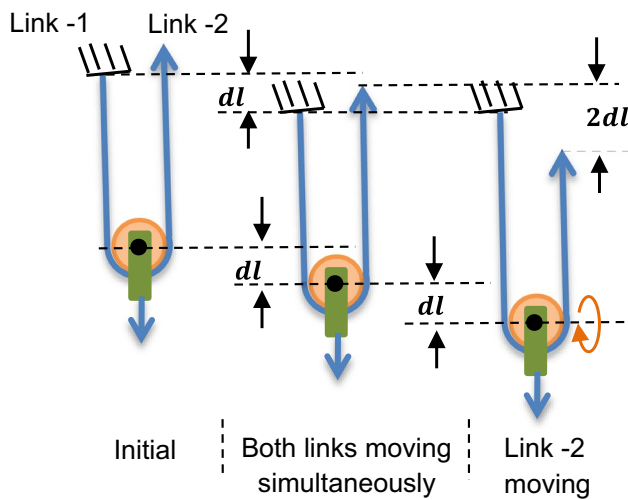


**Fig. 5** Different stages of the movable pulley: initially the movable-pulley is at equilibrium, both the links move simultaneously; once a link stops, the pulley starts to rotate which allows the other link to continue its movement

originating from an actuator or the preceding bifurcation is fixed with the axle of the pulley and a non-stretchable tendon passes over the pulley whose one end is fixed on the immediate link and the other end goes to the next pulley. Initially, the actuation force applied on the pulley produces an equal force on both sides of the tendon passing over the movable pulley. As a result, all the links move simultaneously until it touches an object or the maximum limit is reached. Once a link stops, the rotation of the movable-pulley facilitates the subsequent links to continue their movement. The torque-force relation is decoupled by keeping the pulley  $r_j^2 = 0$  as shown in Fig. 4. So, the relation between the tendon force and joint torque at  $j$ -th joint becomes.

$$\tau_j = r_j^1 f_j^1 \quad (9)$$

Initially, let the linear displacement of the bifurcation-pulley be  $dl$  as shown in Fig. 5, then the relations between the tendon displacements and the joint displacements are as follows.

**Fig. 6** (a) Spiral springs at the joints and the displacement ranges of the proximal and distal joints, (b) The realisation of the single tendon and branching tendon routing paths inside a finger of the two-finger gripper

$$dl_j^1 = dl = r_j^1 dq_j \quad (10)$$

$$dl_j^2 = dl = r_{j+1}^1 dq_{j+1} \quad (11)$$

Once a link touches an object or the maximum limit is reached, the relations between the tendon displacement and the joint displacement are as follows.

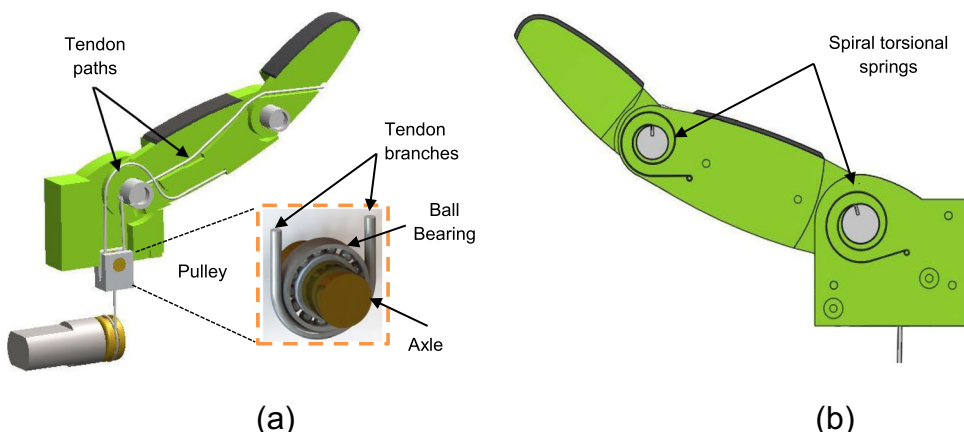
$$dl_j^1 = 0 \quad (12)$$

$$dl_j^2 = 2dl = r_{j+1}^1 dq_{j+1} \quad (13)$$

For the implementation of the actuation mechanism, the bifurcation pulley is realised using a small ball bearing supported by a small movable part. The movable part is connected to the actuator through a tendon wire and moves linearly along the slotted channel inside the knuckle and palm. Another tendon wire passes over the ball bearing attached to the movable part and the two ends of the tendon wire are connected to the links as follows. One of the branches passes over the knuckle-proximal joint pulley and is attached to the proximal link. The other branch runs through the routing path inside the finger and is attached to the distal link. The tendon path and actuation system are shown in Fig. 6(a). The tendon-pulley system only produces flexion motion to the finger, whereas extension motion is achieved using spiral torsional springs at the joints as shown in Fig. 6(b). The pulleys join the links to form an articulated chain from the knuckle to the distal link. The choice of the pulley radius is important because it decides the essential torque that needs to be generated at the joint.

## 2.2 Framework for Optimisation of the Gripper Design and the Tendon Actuation Mechanism

The main focus of the gripper design is to accomplish a stable grasp for a wide range of objects, especially for lightweight objects (e.g. empty plastic bottles) while performing



an envelope/power type of grasp. Then again, it is necessary to ensure that the gripper is not only limited to performing the enveloping type of grasp but is equally effective in realising the fingertip type of grasp. In this regard, a framework for optimisation of the gripper design is presented to select the link dimensions, the pulley radii and the joint springs.

### 2.2.1 Optimisation of Link Dimensions of the Gripper

It is desirable to choose the link dimension in such a way that the gripper is able to wrap its fingers around the object while performing enveloping grasp, in other words, all the links must make contact with an object. Now it can be observed from Fig. 7 that the choice of smaller links may lead to failure in fully wrapping the object, while due to the choice of larger link dimensions, a collision between the fingers may result thus preventing the gripper from making contact with the object.

The starting point for the formulation of the optimisation problem is to define a grasp quality metric for measuring how stably the fingers can grasp the objects. The grasp quality metric proposed by Ferrari and Canny [30] is used for the optimisation of the link dimensions and a brief formulation is given in appendix-B. The volume  $v$  of the convex hull in Eq. 32 gives an invariant measure of grasp quality given that the origin of the wrench space lies within the convex hull. This quality measure is used as a basis for the optimisation of the link dimensions. The optimisation problem is formulated for the knuckle, the middle and the distal links of the proposed gripper. The grasp quality depends on the number of contacts and location on the links, which in turn depend on the link lengths. For example, the grasp as shown in Fig. 7(a) becomes unstable as all the contacts on one side of the object make the origin of the wrench outside the convex hull. In the case of Fig. 7(b), the grasp may become weak as the gripper fails to make contact with all the links. The cumulative grasp quality ( $Q$ ) as given in Eq. 14 over a pool of valid grasps is maximised to find the best link dimensions. A pool of grasps is created from an object database consisting of a set of 3D objects of varied shapes and sizes.

$$Q = \sum_j^N v_j \quad (14)$$

where  $N$  is the size of the grasp pool.

### 2.2.2 Optimisation of the Actuation Mechanism

The main objective of gripper design is to provide a stable grasp by minimising the unbalanced grasping force on the object, which often leads to object ejection from the gripper. The link dimension optimisation only ensures that the gripper will be able to fully wrap a wide range of objects, whereas the unbalanced grasping force on the object can

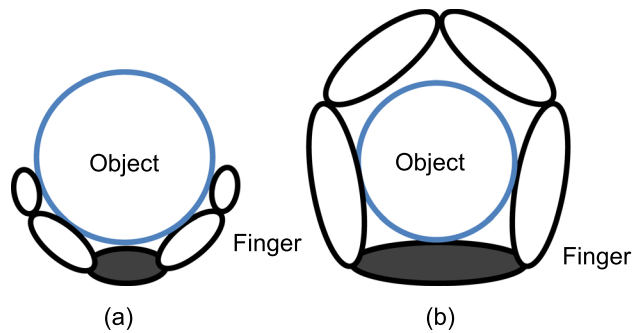


**Fig. 7** (a) Fingers with smaller links fail to fully wrap the object (b) fingers with larger links collide with each other

be minimised by optimising the actuation mechanism. The pulley radii and joint spring stiffness are the main design parameters, which decide the behaviour of the mechanism and are considered for optimisation. The optimisation of the actuation system is a two-step process as formulated below. In the first step, the pulley ratio between the proximal and distal pulleys is determined based on the joint displacement data. In the second step, the pulley radii and joint spring stiffness are determined by formulating the grasp stability as an optimisation problem and minimising the unbalanced grasping force over an object dataset.

The best way to prevent object ejection from the gripper is to close the fingers in such a way that all the links make contact simultaneously as discussed earlier. Now, the pulley ratio decides the joint displacement of the distal to the proximal joint, in other word, how quickly the distal link closes relative to the proximal link. The choice of a small pulley ratio results in an unbalanced contact force as only proximal links can make contact with the object which leads to grasping failure, while a large ratio makes the distal links touch the object without proximal link contacts which results in a weak grasp as shown in Fig. 8. The pulley ratio can be defined for the  $i$ -th and  $(i+1)$ -th joints as follows.

$$\gamma = \frac{r_i}{r_{i+1}} \quad (15)$$

So, it is important to choose the pulley ratio in such a way that it fits a wide range of objects. The idea is to use joint displacement data to estimate a model for the pulley radii ratio to avoid the two extreme cases as shown in Fig. 8 and try to find a suitable configuration for a wide range of objects. Here for implementing the idea, linear regression is used to estimate the pulley ratio over a pool of grasps consisting of a wide range of objects.

In the next step of optimisation, first the mathematical relation between the grasp stability with the optimisation parameters is established and then appropriate optimisation method is chosen. Now, the generated torques at the joints by the tendon forces as shown in Fig. 4 can be written as.

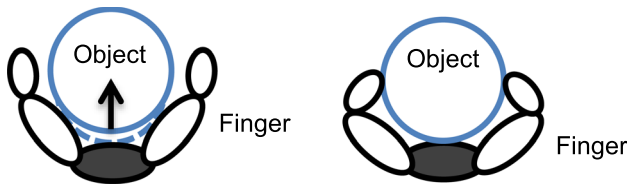


**Fig. 8** Fingers make contacts with the object (left), quick closure of the distal link leaves no time for proximal links to make contacts (right)

$$\boldsymbol{\tau} = \mathbf{R}\mathbf{f} - \mathbf{K}\mathbf{q} \quad (16)$$

where,  $\mathbf{R}$  is constructed from pulley radii vector  $\mathbf{r}$  and  $\mathbf{K}$  is a diagonal matrix of spring stiffness vector  $\mathbf{k}$ .

The stability analysis of grasp given in the work by Ciocarlie and Allen [31] is used as a basis for the second step i.e., the optimisation of pulley radii and joint spring stiffness. The formulation states that a grasp is in equilibrium if the following conditions are satisfied: the contact forces must be balanced by joint torques; the resultant contact wrench on the object through the contacts by the fingers is null; all the contact constraints are met (e.g., positive normal components and friction constraints). Let the gripper establish a total of  $n$  number of contacts with an object. Then the above conditions can be expressed as follows.

$$\mathbf{J}_h^T \mathbf{D} \boldsymbol{\beta} = \boldsymbol{\tau} \quad (17)$$

$$\mathbf{G}\boldsymbol{\beta} = 0 \quad (18)$$

$$\boldsymbol{\beta}, \mathbf{F}\boldsymbol{\beta} \geq 0 \quad (19)$$

where,  $\boldsymbol{\tau}$  is the joint torque vector,  $\mathbf{J}_h$  and  $\mathbf{G}$  are gripper Jacobian matrix and the grasp matrix respectively,  $\boldsymbol{\beta}$  is the force vector containing the contact force components of all contacts in block column vector form,  $\mathbf{D}$  is the selection matrix depending on the type of contact modelling (e.g., point contact with friction or without friction, soft contact, etc.) and  $\mathbf{F}$  matrix is related to the friction model (e.g., linearized Coulomb friction), these  $\mathbf{D}$  and  $\mathbf{F}$  matrices are constructed by assembling all individual contact constraint matrices for  $n$  contacts in block diagonal form (more details can be found in the work by Ciocarlie and Allen [31]).

The torque relation given by Eq. 16 can be rewritten in the following linear form of design parameters  $\mathbf{r}$  and  $\mathbf{k}$ , where the tendon force vector  $\mathbf{f}$  is normalised to the unit vector (maximum gripper closing force).

$$\boldsymbol{\tau} = \mathbf{P}\mathbf{r} + \mathbf{Q}\mathbf{k} \quad (20)$$

where  $\mathbf{P}$  and  $\mathbf{Q}$  depend on the normalised tendon forces and the normalised joint displacements, respectively.

Similar to the previous sub-section, a pool of valid grasps over an object database is used for formulating the optimisation problem. For the  $j$ -th grasp in the pool, by combining Eqs. 17 and 20 the conditions for the gripper to be in equilibrium with the object can be written as follows.

$$(\mathbf{J}_h^j)^T \mathbf{D}^j \boldsymbol{\beta}^j = \mathbf{P}^j \mathbf{r} + \mathbf{Q}^j \mathbf{k} \quad (21)$$

$$\mathbf{G}^j \boldsymbol{\beta}^j = 0 \quad (22)$$

$$\boldsymbol{\beta}^j, \mathbf{F}^j \boldsymbol{\beta}^j \geq 0 \quad (23)$$

where pulley radii  $\mathbf{r}$  and joint spring stiffness  $\mathbf{k}$  are independent of the grasp pool and are shared by all the grasps in the pool.

The Eqs. 21, 22 and 23 are assembled in block matrix form over the grasp pool to formulate the optimisation problem as a quadratic optimisation problem as follows

$$\text{minimise} \left\| \begin{bmatrix} \mathbf{J}_h^T \mathbf{D} - \bar{\mathbf{P}} - \bar{\mathbf{Q}} \\ \mathbf{r} \\ \mathbf{k} \end{bmatrix} \right\| \quad (24)$$

subject to constraints

$$\bar{\mathbf{G}}\bar{\boldsymbol{\beta}} = 0 \quad (25)$$

$$\bar{\boldsymbol{\beta}}, \bar{\mathbf{F}}\bar{\boldsymbol{\beta}} \geq 0 \quad (26)$$

$$\mathbf{r}_{min} \leq \mathbf{r} \leq \mathbf{r}_{max} \quad (27)$$

$$\mathbf{k}_{min} \leq \mathbf{k} \leq \mathbf{k}_{max} \quad (28)$$

where the matrices  $\bar{\mathbf{J}}_h^T, \bar{\mathbf{D}}, \bar{\mathbf{P}}, \bar{\mathbf{Q}}, \bar{\mathbf{G}}, \bar{\mathbf{F}}$  are assembled in block diagonal form, while  $\bar{\boldsymbol{\beta}}$  is in block columns form of the contact forces for individual grasp in the pool.

### 2.3 Development of the Proposed Grippers

Firstly, the design parameters of the proposed gripper have been optimised for grasping objects of different geometric shapes based on the approach discussed in Sect. 2.2. A soft computing based global optimisation algorithm, Simulated Annealing (SA) [32], has been applied to optimise the link dimensions of the fingers, whereas quadratic programming [33] has been used for the actuation mechanism optimisation. The limits of the link lengths, pulley radius and spring stiffness constant for the gripper are given in Table 1. The limits of the link lengths and pulley radius are chosen based on the physical limitations (i.e. space required for joint pulleys, sensors and actuators) and also after several optimisation trials by using different combinations of link limits.

**Table 1** Lower and upper limits of the link lengths, pulley radius and spring stiffness for the gripper

	Knuckle link length $l_1$ (mm)	Proximal link length $l_2$ (mm)	Distal link length $l_3$ (mm)	Pulley radius $r$ (mm)	Spring stiffness $k$ (N-mm/rad)
Minimum	25	45	25	6	15
Maximum	45	75	45	9	50

Here two factors are considered for the choosing the limit values of the spring stiffness constant. First, the spring should able to keep the finger extended state position against its own weights when no actuation force is applied. Secondly, as it acts against the actuation force so, high spring stiffness reduces the effective actuation force resulting in low gripping force. Considering these two factors, upper and lower limits of spring stiffness have been set.

For the link dimensions, the mean values of the link limits set the seed values of the optimisation variables and other parameters of the SA. In each iteration of SA, the new solutions of the optimisation variables are generated using random Gaussian distribution. A dataset of common household objects taken from the Princeton Shape Benchmark[34] and the KIT dataset [35] has been used for generating a pool of grasps consisting of 760 grasps. The grasps on each object in the above dataset are generated using the object-slicing based grasp planner [36]. Then the best link lengths are found by maximising the cumulative grasp quality over the aforementioned grasp pool. Different combinations of parameter values have been used for the implementation of the SA algorithm as follows: the cooling rate  $\alpha$  is in the range of 0.83–0.9; the initial temperature  $T_0$  is in the range of 30–100; the stopping criterion  $\epsilon$  is of 0.1; the mean  $\mu$  and standard deviation  $\sigma$  of the Gaussian distribution are initialised with the initial link lengths and updated with the current link length values, i.e. optimisation variables, after

every iteration. The convergence plots for two such instances with  $T = 30$  and  $\alpha = 0.83$  are shown in Fig. 9. Initially, the cumulative grasp quality ( $G$ ) keeps changing then as the temperature decreases, it converges to the global maximum value. It can be seen from the plots that the convergence of the optimisation algorithm is achieved in about 160–200 iterations. For the two-finger gripper, the optimised lengths of the knuckle, proximal and distal links are found to be 34.2 mm, 58.4 mm and 44.4 mm respectively.

Further for the actuation mechanism optimisation, the joint pulley ratio  $\gamma$  is estimated from the joint displacement data of the found grasps over the same object dataset as mentioned above. The joint ratio  $\gamma$  relates the proximal joint pulley to the distal joint pulley, whereas the same stiffness value is considered for both the joints of each finger. So for the implementation of the quadratic programming, the optimisation variable vector of the cost function in Eq. 24 contains only one pulley radii  $r$ , one stiffness constant  $k$  and the contact forces  $\beta$ . The linear regression technique estimates the pulley ratio  $\gamma$  of 1.3 over the pool of grasps. The optimised pulley radii and spring stiffness are found to be 9 mm and 15 N-mm/rad respectively. It can be seen from the results that these values are the upper and lower boundaries of the pulley radii and the spring stiffness respectively. This is related to maximising the effective actuation force from the actuator to grasping force by bigger pulleys and softer springs.

**Fig. 9** The convergence plots of the simulated annealing algorithm for different values of temperature and cooling rate

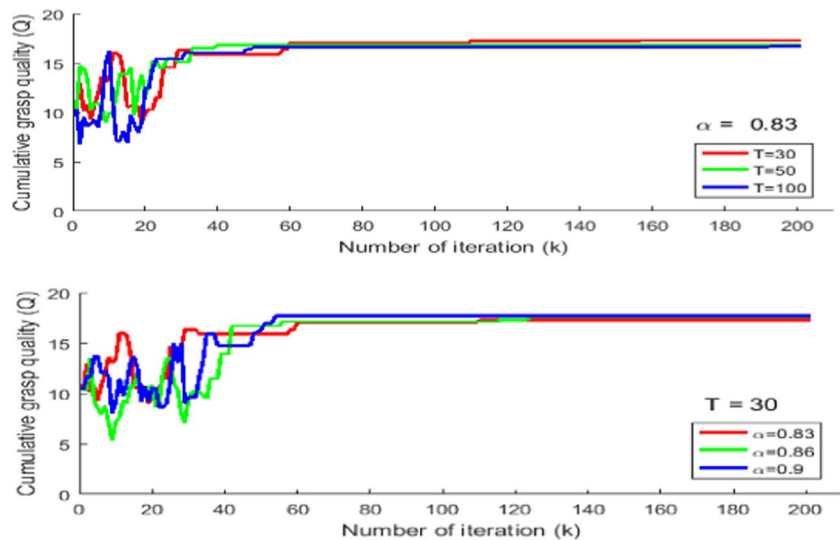




**Fig. 10** The 3D printed prototype of the two-finger gripper

### 2.3.1 Fabrication of the Grippers

The physical prototype of the gripper as shown in Fig. 10 has been manufactured using 3D printing which has reduced the overall design and development time. Polylactic acid, a thermoplastic commonly known as PLA, is used for printing. The lengths of the knuckle, proximal and distal links for the two-finger gripper are 34 mm, 58 mm and 44 mm respectively. The overall weight of the gripper is 200 g, whereas the individual weights of the knuckle, proximal and distal links are 12 g, 10 g, and 5 g respectively. The printed finger surface is smooth and provides very little friction while grasping objects. Further, the rigid and hard surfaces also provide very little contact area between the fingers and the object surface. To make the contact area larger for helping to distribute grasping force over a larger contact surface on the object and to stabilise the grasps, a thin layer of padding made of rubber is provided on the contact areas of the fingers as well on the palm surface.

Several materials have been tried for the tendons such as polyester, nylon and steel strings. In the final prototypes,

threaded strings made of polyester have been used for the tendons. The string is lightweight and has a tensile strength of 12 kg with a diameter of 0.4 mm. The joint springs are made of flat stainless-steel strips, which are available in different thicknesses and widths. The spring strip with a thickness of 0.25 mm and width of 1 mm has a spring constant of 17.8 N-mm/rad, which is closest to the optimised stiffness constant value of 15 N-mm/rad and has been used for joints.

The exploded views of the gripper showing the assembly directions, labelling of parts, and the quantities of each component needed to manufacture are presented in Fig. 11. All the parts, except the screws, motors, PCB, magnets, padding and bearing, are 3D printed as shown in Fig. 11. The design is modular so that each finger is assembled separately and fitted to the palm.

### 2.3.2 Actuator and Sensor Integration

The major challenges of choosing an appropriate motor for finger actuation are the limited physical space available within the finger and the high degree of required torque. Small dc motors are chosen as shown in Fig. 12(a), which can generate maximum rated output torque of 0.00569 Nm and can achieve a rotational speed of 1200 rpm. The motors have an integrated gearbox with a gear ratio of 100:1 and a pulley is fixed on the output shaft for driving the tendon wires. The two small dc motors are placed inside the palm, one motor for actuating each finger as shown in Fig. 12(a) and the motors are controlled by using double H-bridge based motor drivers.

Hall-effect based contactless sensors are used at the joints as well as at the motors, which measure the angular displacements of the fingers and rotation of the motors. The sensor consists of a small permanent two-pole magnet and a hall-effect based integrated circuit (IC) chip. The sensor provides absolute angular displacement of the magnet rotating above

**Fig. 11** The exploded views of the finger sub-assembly and the gripper assembly

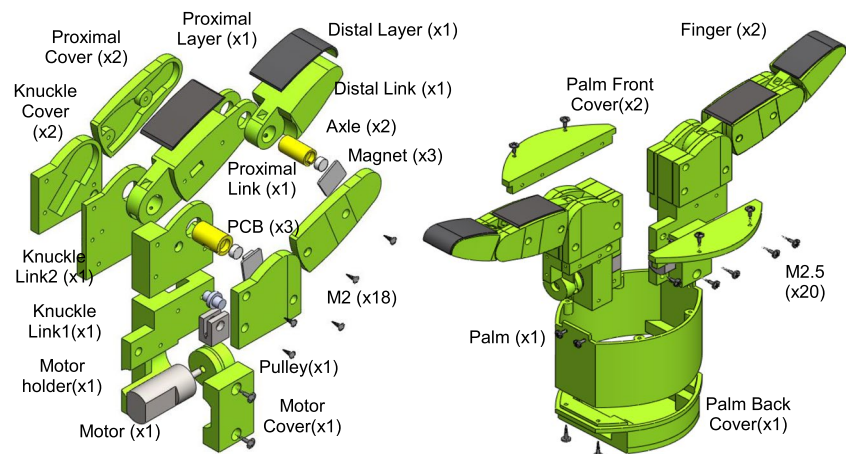
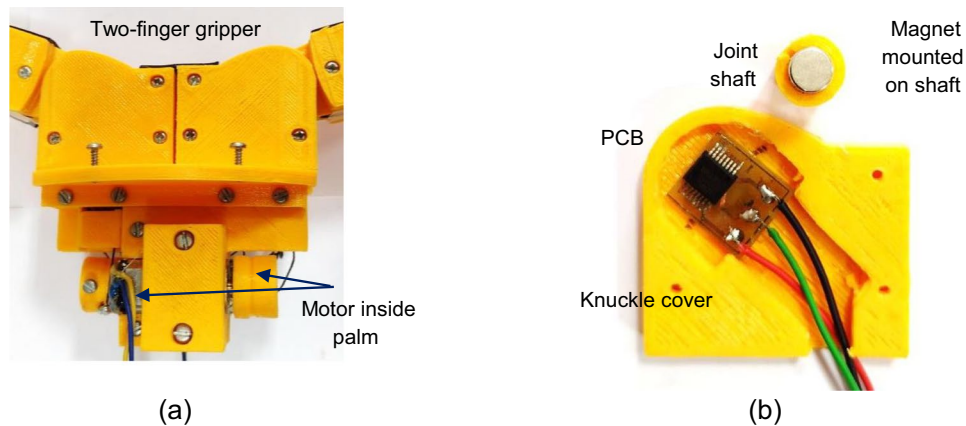


**Fig. 12** (a) Actuator installation inside the gripper palm and (b) installation of the chip and magnet in the knuckle joint of the gripper finger



the centre of the chip over a full turn of 360 degrees with a resolution of  $0.0879^\circ$  or 4096 positions per revolution. The chip is surface mounted on a small printed circuit board (PCB) as shown in Fig. 12(b) and placed at each joint. The magnet is mounted on the shaft of the joint pulley as shown in Fig. 12(b).

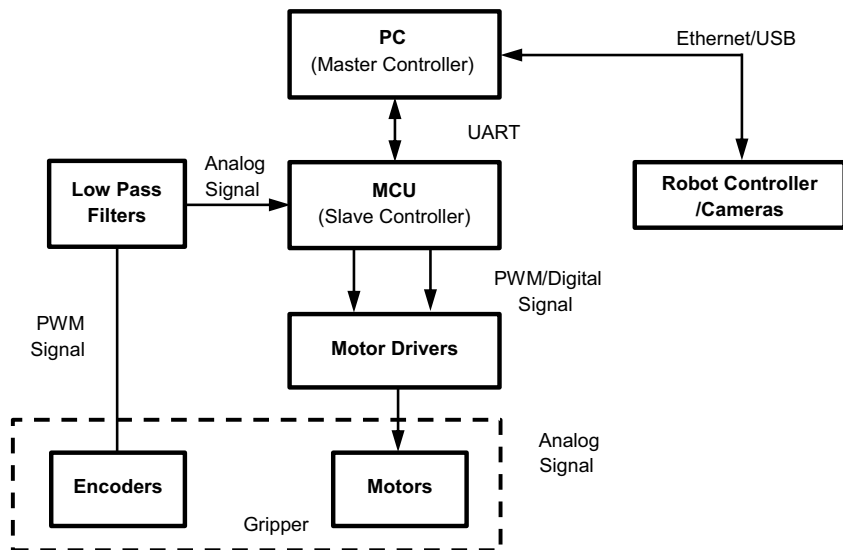
### 2.3.3 Hardware Implementation of the Gripper Controller

The controller architecture of the grippers is of master and slave configuration, where a PC acting as master communicates with the slave microcontroller unit (MCU) and other units (e.g., in case of full system integration, the robot controller and the 3D cameras through Ethernet and USB respectively) as shown Fig. 13. A user (or the grasp planner in the case of an automated grasping system) can interactively send grasping commands to the gripper using a graphical user interface (GUI) running on the master PC. The lower level of control algorithm runs on the MCU and it communicates with the master PC through the serial

Universal Asynchronous Receiver Transmitter (UART) port. The MCU computes the required motor actuation and directions for executing the grasping command from the master PC. The MCU uses analog and digital I/O ports to send the signal to motor drivers and receives the feedback signal from encoders. The motor drivers supply the required current to the motors. The output of the encoders is in the form of a PWM signal, so low pass filters are used to convert the PWM to analog signals.

The hardware implementation of the gripper controller architecture is shown in Fig. 14. An Arduino Uno board acts as the slave controller, which is an open-source MCU based on the microcontroller chip ATmega328P. The GUI is developed on the MATLAB app designer, which interactively takes inputs from the user or the grasp planner. The current version of the GUI has two options for user inputs as shown in Fig. 14. Firstly, the user can simply open or close the gripper by pressing the ‘Open’ or ‘Close’ button. Secondly, the user can select joint displacement values using the sliders and then press ‘Move’ button to move the fingers.

**Fig. 13** Flowchart of the controller architecture of the grippers



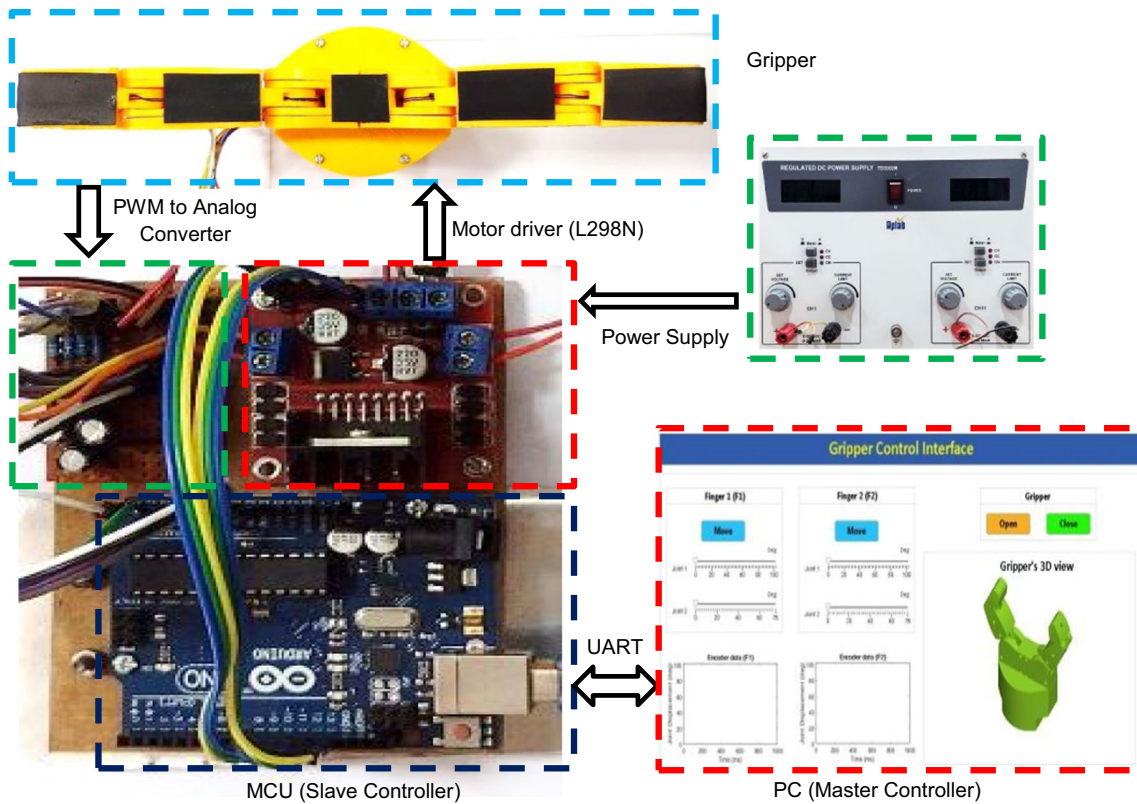


**Fig. 14** Hardware implementation of the gripper controller

It also has the option to visualise the joint displacement outputs as well as the gripper movements in real-time. The GUI uses the feedback from the joint encoders to continuously update the 3D view of the gripper and also plot the joint displacement in real-time.

### 3 Experimental Results and Discussions

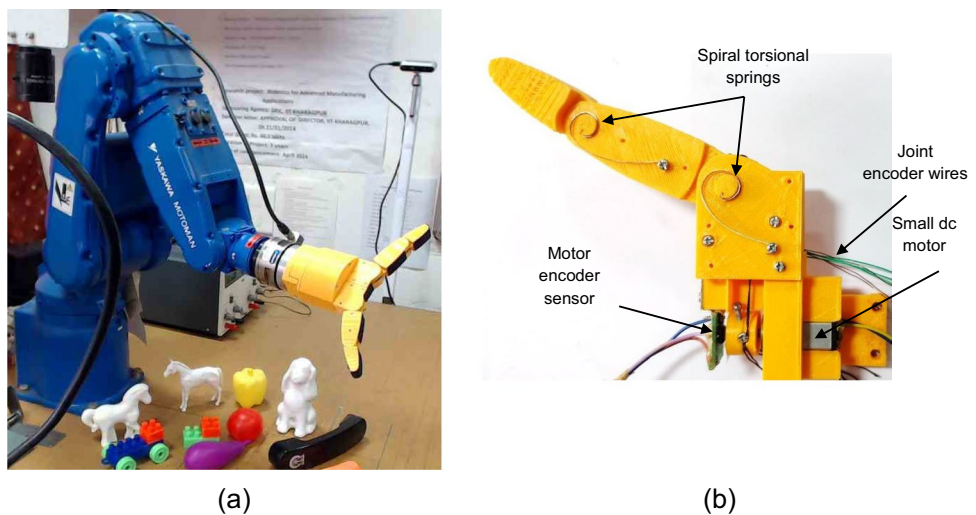
Experiments have been conducted using the developed two-finger adaptive gripper for performing grasp operations by mounting them on the wrist of a Motoman industrial robot as shown in Fig. 15(a). Moreover, an experimental setup consisting of a single finger has been developed for studying the actuation mechanisms and the finger motion as shown in Fig. 15(b). Further, a position-based impedance controller has been implemented on the MCU for studying the finger motion. The position-based impedance controller is designed on top of a PID controller as more details given in appendix-C. The coefficients of the PID block and the impedance stiffness are found to be of  $K_p = 1.5$ ,  $K_i = 1$ ,  $K_d = 0.009$  and  $K_s = 0.3 \text{ Nm/rad}$ , where  $K_p$ ,  $K_i$ ,  $K_d$ , and  $K_s$  are proportional, integral, derivative and, impedance stiffness constants respectively. The mass of the knuckle, proximal and distal links are 12 g, 10 g, and 5 g respectively.

#### 3.1 Finger Motion for the Tendon-Driven Actuation Mechanism

The experimental results of finger motion for the tendon branching mechanism are shown in Figs. 16 (a) and (b). The tendon branching mechanism exhibits the desired level of joint movements for the finger to be shape adaptive.

It can be seen from the results that both the link start moving simultaneously in the absence of external as shown in Fig. 16(a). In the presence of an object, the distal link continues to move once the proximal link is stopped by making contacts with the object as shown in Fig. 16(b). The joint encoder values and tendon displacement plots for the two cases (i.e., without external constraints and with constraints) are shown in Figs. 17 and 18 respectively, where same results as Fig. 16 can be seen. In case of no external constraints, both the proximal and distal joint displacements increase simultaneously until maximum joint limits are reached. In the presence of external constraints, initially both joint displacement values increase and only distal joint value changes after proximal links making contact with the object as shown in Fig. 18. The tendon displacement curves are plotted using the data collected from the motor encoder. The joint displacement ratio curve for the proximal and distal joints of the finger is computed using the joint encoder

**Fig. 15** (a) The developed gripper mounted on the wrist of Motoman industrial robot, (b) An experimental setup consisting of a single finger



data as shown in Fig. 19, which is closely following the desired ratio of 1.3.

### 3.2 Object Grasping Test for the Actuation Mechanism

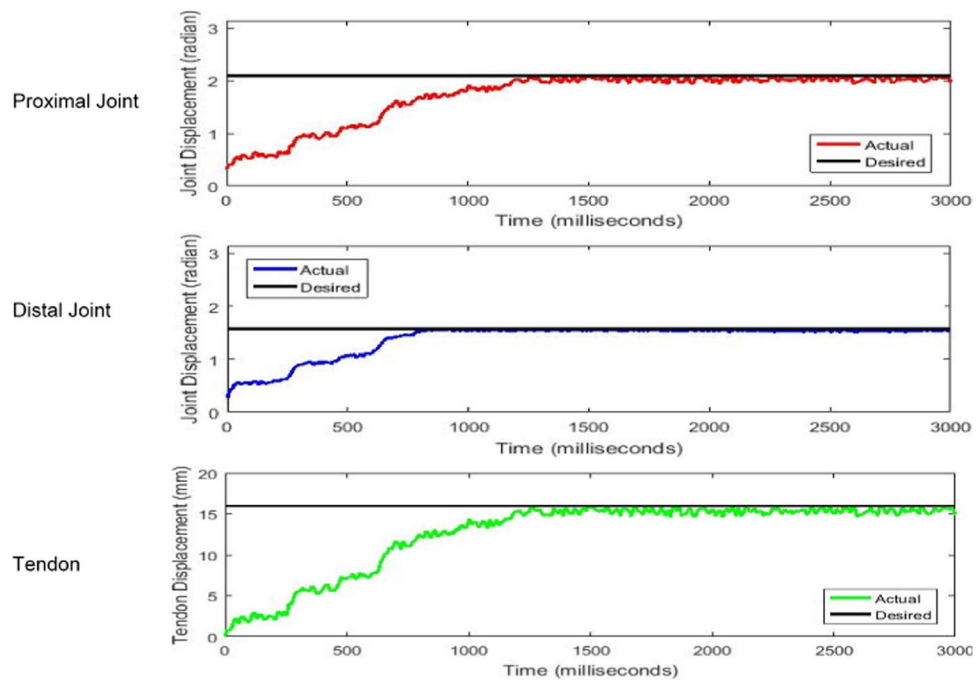
The proposed mechanism has been put to test by executing object grasping using the developed two-finger gripper. The gripper has been mounted on a Motoman industrial robot manipulator for performing simple pick and place operations. Here for illustrating the object ejection problem, a single tendon mechanism [25] is also implemented on the gripper, where the first link starts to move when actuation force is applied and the subsequent links only move once the precedent link touches an object or maximum joint limit reached as shown in Fig. 2(a). The examples of grasping

a few lightweight real objects in the range of 10–50 g of weight by the developed gripper for both the actuation mechanisms are shown in Figs. 20 and 21. For the single tendon mechanism, the two-finger gripper fails to grasp the empty bottle as the proximal links continuously push the bottle away without the support of distal links which only start to move once the proximal links are stopped and eventually, it fails to prevent the fall of the object as shown in Figs. 20(a). But it successfully grasps the bottle filled with water as the proximal links are stopped after making contacts with the heavier bottles and then only the distal links are able to move resulting in fingers enveloping the object as shown in Fig. 20(b). In the case of the developed tendon branching mechanism, the simultaneous closing of proximal and distal links helps the gripper to successfully grasp the empty bottle as well as the filled bottle as shown in Fig. 21.



**Fig. 16** (a) The simultaneous closing motion of the two links without external constraints, (b) Continuation of motion of the second link after the first link is stopped by touching an object

**Fig. 17** The trajectory of the proximal and distal joints with simultaneous closing of both the finger joints without external constraints



The grasping test has been performed five times on each object by using the gripper with both the tendon branching mechanism as well as with the single tendon mechanism. The numbers of successful grasps out of those five tests are shown in Fig. 22 with the help of a bar graph. The bars with colour blue and yellow show the number of successful grasps for the tendon branching mechanism and the single tendon mechanism respectively.

It can be seen from the figure that the success rate has improved significantly for the tendon branching mechanism while performing the envelope type of grasp. It is to be noted that the experiment is performed on two different bottles with different surface conditions. The surface of the first bottle is less smooth than the second one resulting in some grasp success for the single tendon mechanism. The single tendon mechanism performs the

**Fig. 18** The trajectory of the proximal and distal joints and the tendon displacement with simultaneous closing of both the finger joints with external constraints

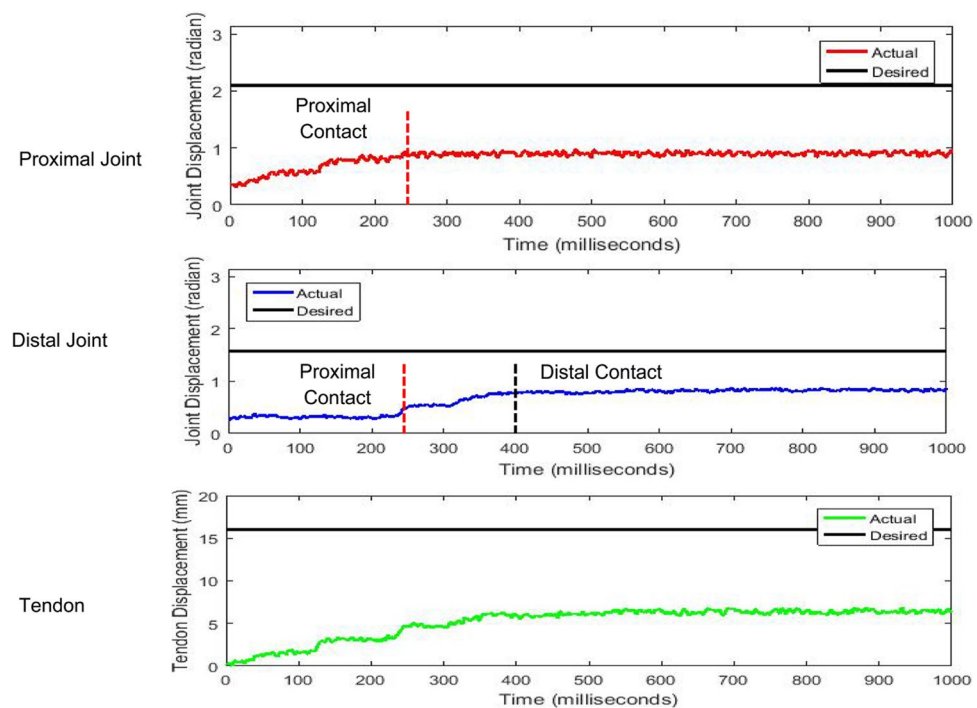
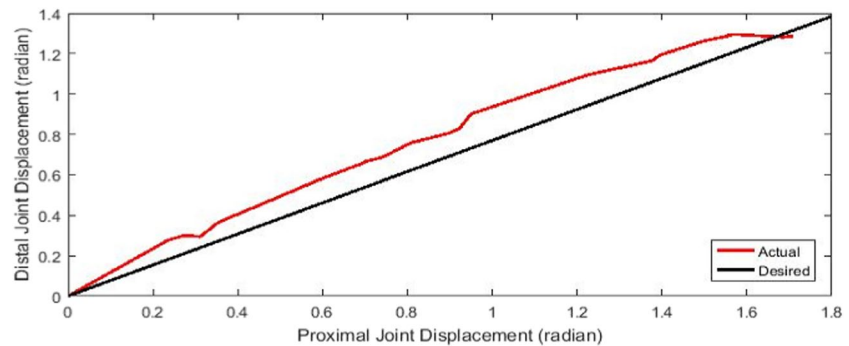


**Fig. 19** The joint displacement ratio curve for the proximal and distal joints of the finger with tendon branching mechanism



poorest for the bottles. Further, it can be noticed that the single tendon mechanism performs marginally better for small objects or in the case of the fingertip type of grasp. This is because the fingers remain parallel producing relatively more contact area with the object for the fingertip type of grasps in the case of the single tendon mechanism.

### 3.3 Effects of the Optimisation on the Grasping Performance

In the initial phase of design and prototype development, a two-finger gripper was developed without design

optimisation. The lengths of the knuckle, proximal and distal links for the un-optimised gripper are 28 mm, 50 mm and 30 mm respectively. The experiment results on this un-optimised gripper have chosen to show the relevance of the optimisation framework. An instance of grasping a very lightweight object from the dataset is shown in Fig. 23 for both the optimised and un-optimised grippers. The shorter fingers of the un-optimised gripper fail to fully wrap around the object resulting in a grasp failure, while the optimised gripper successfully grasps the object. The optimised gripper succeeds in fully wrapping around all the objects in the dataset, while the un-optimised gripper either fails to fully

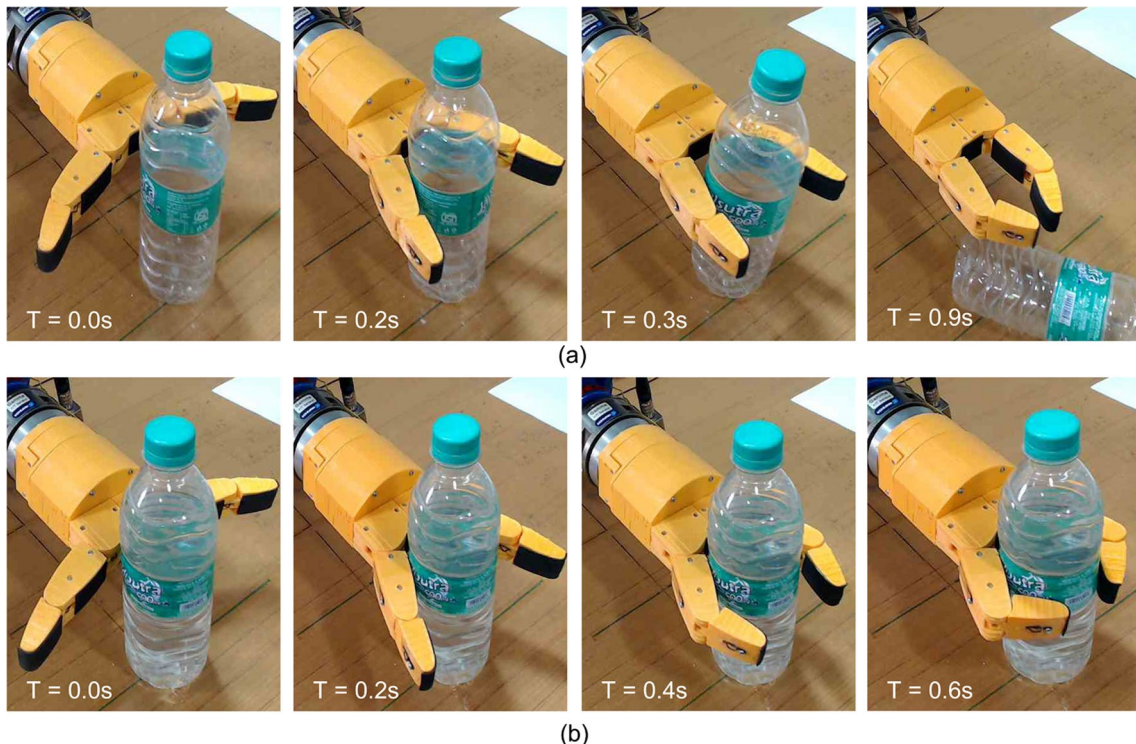


**Fig. 20** Examples showing (a) unsuccessful grasp in case of an empty bottle and (b) successful grasp in case of a bottle filled with water using the gripper with single tendon

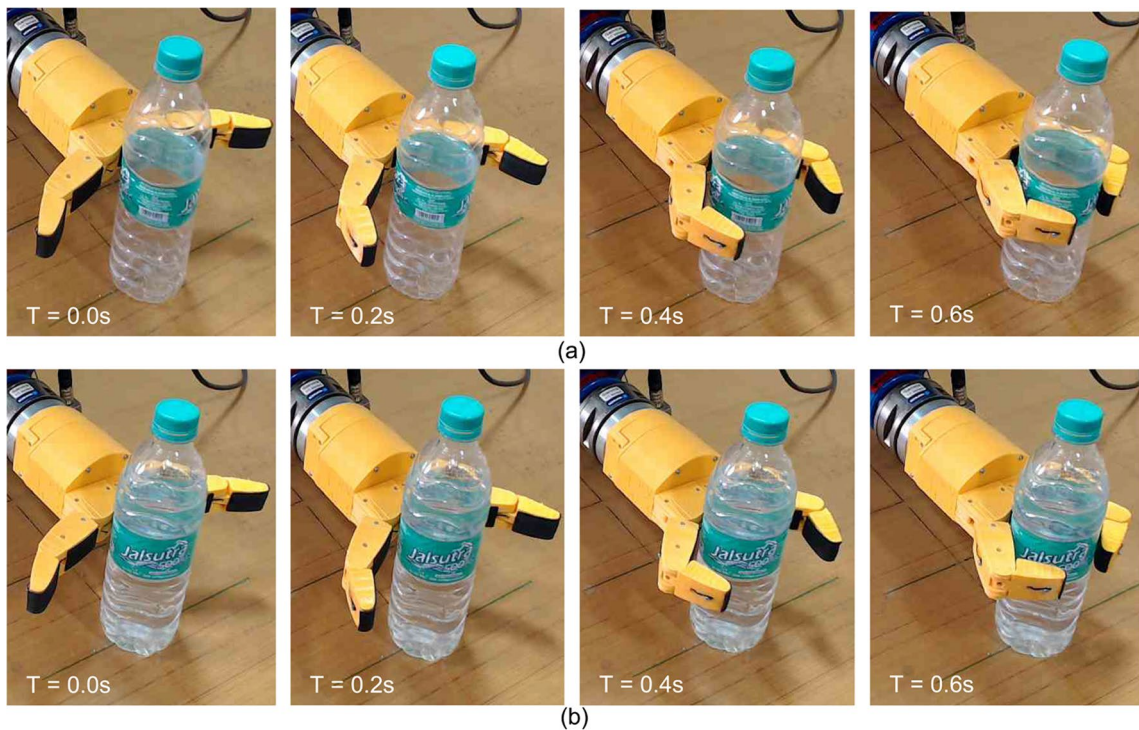
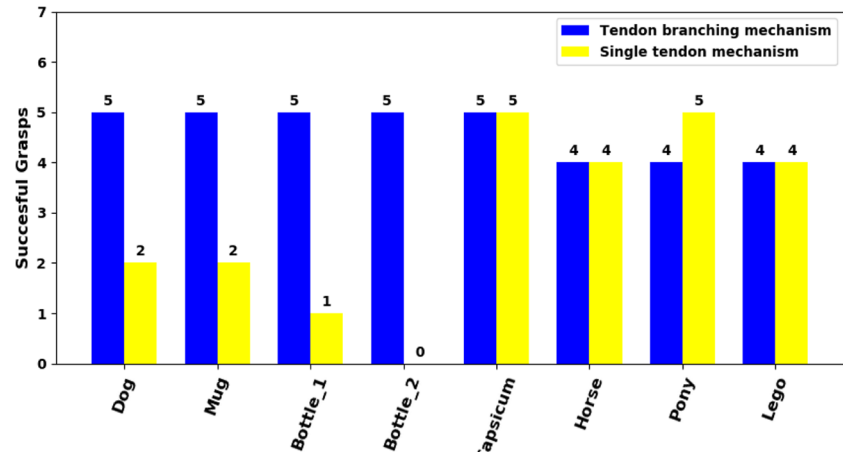


**Fig. 21** Examples showing successful grasps for both the cases of (a) a lightweight empty bottle and (b) a bottle filled with water using the gripper with tendon branching mechanism

wrap around the objects bigger in size or partially wraps around the medium size objects resulting in a weak grasp e.g., the dog and the mug. The numbers of successful grasps out of five tests for each on a subset of eight objects using the optimised and un-optimised grippers are shown in Fig. 24. It is also found that the un-optimised gripper produces weak grasping force due to the high spring constant values, which are two times higher than the optimised spring constant, resulting in grasp failures e.g., the bottle filled with water. It

is noted that the un-optimised gripper can grasp the capsicum\* using enveloping type of grasp (resulting in a higher grasp rate as shown in Fig. 24) due to shorter finger length as well as using fingertips, while the optimised gripper can only grasp it by fingertips. Moreover, the distal link closes at a higher rate (since both the joint pulleys have an equal diameter of 16 mm) producing a weak grasp in the case of the un-optimised gripper at the time of fingertip type of grasp e.g., the pony and the lego.

**Fig. 22** The number of successful grasps out of the top five grasps from the grasp pool



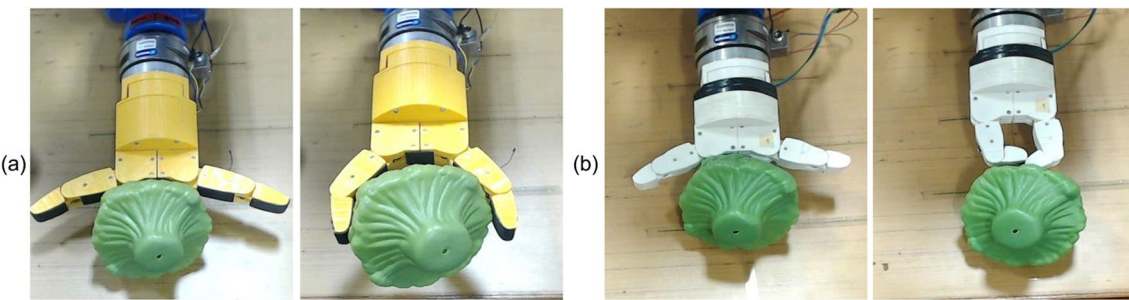


**Fig. 23** Examples showing (a) successful grasp by optimised a gripper and (b) unsuccessful grasp by un-optimised a gripper

### 3.4 Object Grasping Using the Developed Two-Finger Adaptive Gripper

The grasping operation is performed on the same set of objects used for the design optimization. The results for a sub-set of real objects are shown in Fig. 25 using the developed gripper. It can be seen from the figure that the gripper is capable of performing adaptive/enveloping as well as fingertip grasps.

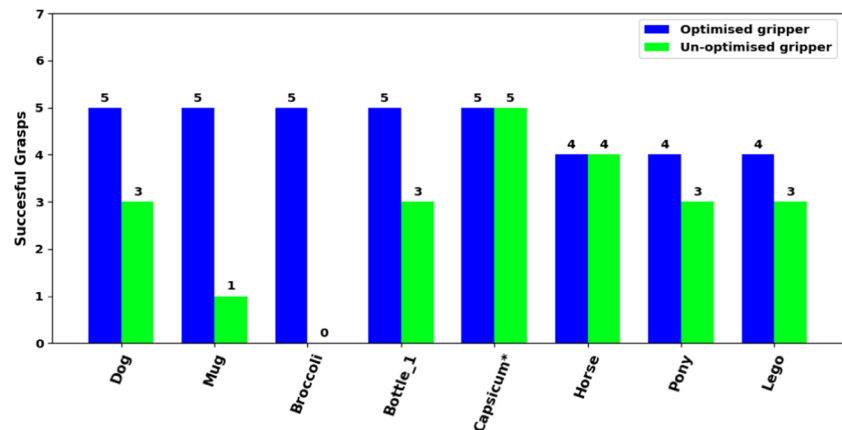
## 4 Conclusions

In this work, a simple adaptive actuation mechanism based on a movable pulley and tendons has been designed. It is found that the developed actuation mechanism exhibits the desired level of joint movements for the finger to be shape-adaptive. The optimisation of the design parameters has been done over a dataset of common household objects. A two-finger gripper based on the optimisation results has been developed using 3D printing technology, which can perform adaptive/enveloping as well as fingertip grasps. Further, Magnetic position sensors are

incorporated at each joint of the fingers for measuring joint displacements and also embedded for measuring the motor rotation. Finally, the proposed mechanism is validated by performing a pick and place operation on an industrial Motoman robot and the developed gripper. It is found that the simultaneous closing of proximal and distal links helps the gripper to successfully grasp lightweight objects.

Although the developed adaptive gripper is able to perform a fingertip type of grasp, the grasp may be weak due to relatively lesser contact area for small objects as compared to a parallel gripper. To address this limitation, one may explore the possibility of increasing the number of finger links and making arrangements to keep the distal links parallel. The gripper designs and actuation mechanisms found in the literature are very diverse. It could be a very interesting research work to develop a generalised metric to quantify the design complexity of different gripper mechanisms. Further, the use of different tactile and torque/force sensors can be explored to improve the gripper controllability. The controller design is out of the scope for the current work, but will be considered for the future work.

**Fig. 24** The number of successful grasps out of the top five grasps for both the optimised and un-optimised grippers



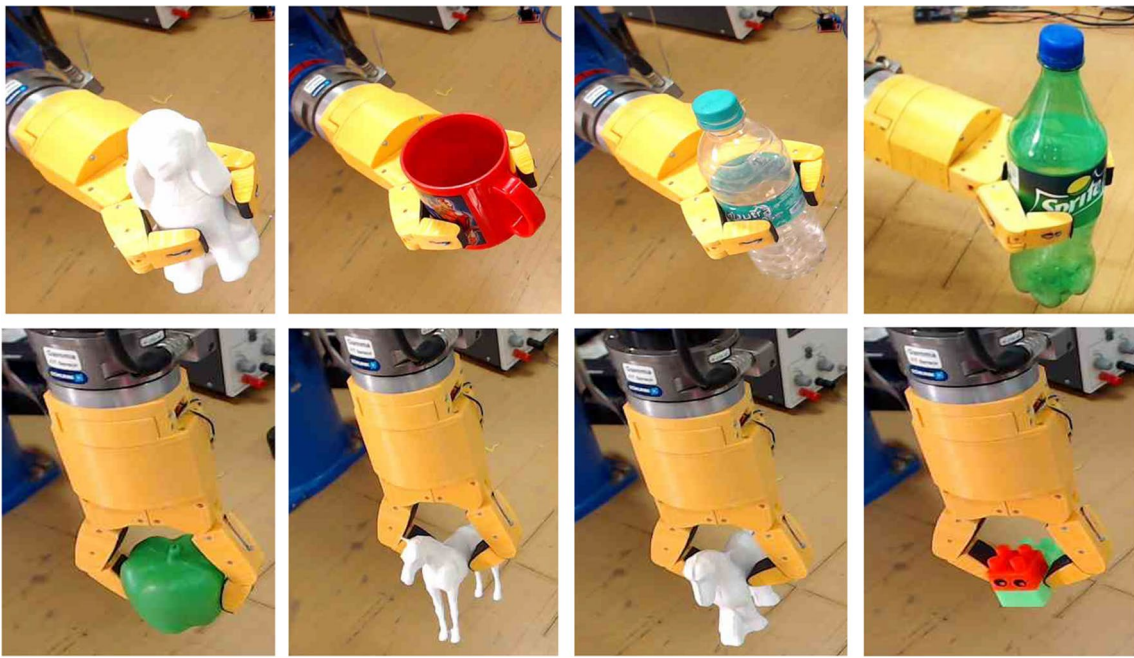


**Fig. 25** Examples of successful grasping operations performed on a few real objects by the two-finger gripper

## Appendix

### A. Kinematics of the Gripper

See Fig. 26

The kinematics for the fingers is determined using the Denavit-Hartenberg (DH) notation. With the convention of DH frame assignments, the reference frames are attached to the links of the fingers, where the Z-axis of link frame

coincides with the joint axis as shown in Fig. 26. The frames are denoted as  $[X_k Y_k Z_k]$ , where the subscript {k} is the link number starting with {k = 0} for the fixed knuckle link. The DH parameters for both the fingers are given in Table 2, where the four DH parameters denoted as  $\alpha_{k-1}$ ,  $a_{k-1}$ ,  $d_k$  and  $\theta_k$  are for the interconnection between link  $k - 1$  and link  $k$ .

The forward kinematics relationship between frame {0} and the fingertip frame {3} is determined by using the DH parameters given in Table 2 as follows.

**Fig. 26** Kinematics schematic with parameter annotations and frame assignments for the two-finger gripper

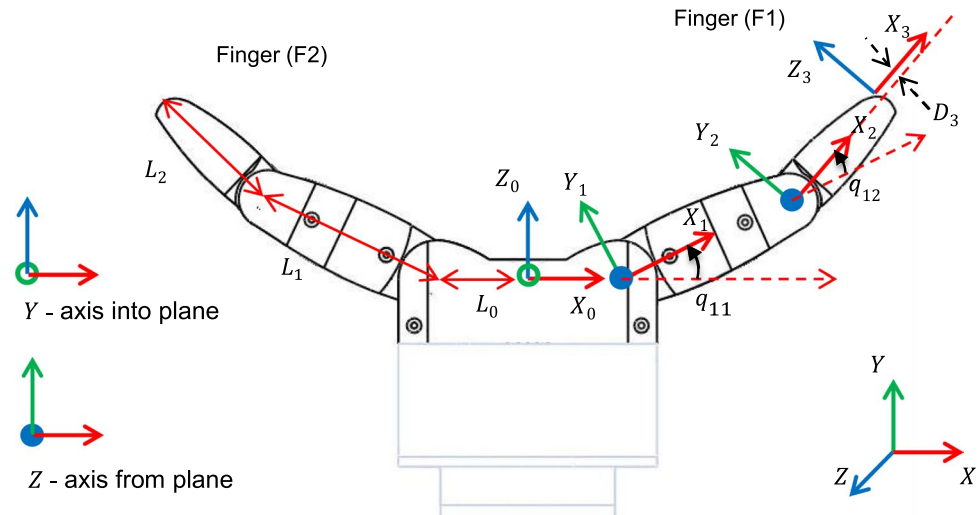


**Table 2** DH parameters for both fingers of the two-finger gripper

Finger (F1)					Finger (F2)				
k	$\alpha_{k-1}$	$a_{k-1}$	$d_k$	$\theta_k$	k	$\alpha_{k-1}$	$a_{k-1}$	$d_k$	$\theta_k$
1	$\pi/2$	$L_0$	0	$q_{11}$	0	0	0	0	$-\pi$
2	0	$L_1$	0	$q_{12}$	1	$\pi/2$	$L_0$	0	$q_{21}$
3	$-\pi/2$	$L_2$	$D_3$	0	2	0	$L_1$	0	$q_{22}$
					3	$-\pi/2$	$L_2$	$D_3$	0

$${}_3^0T = \begin{bmatrix} r_{11} & r_{12} & r_{13} & p_x \\ r_{21} & r_{22} & r_{23} & p_y \\ r_{31} & r_{32} & r_{33} & p_z \\ 0 & 0 & 0 & 1 \end{bmatrix} \quad (29)$$

where, the matrix elements for the finger (F1) are as follows

$$p_x = \cos(q_{11} + q_{12})L_3 - \sin(q_{11} + q_{12})D_3 + \cos(q_{11})L_1 + L_0$$

$$p_y = 0$$

$$p_z = \sin(q_{11} + q_{12})L_3 + \cos(q_{11} + q_{12})D_3 + \sin(q_{11})L_1$$

$$r_{11} = \cos(q_{11} + q_{12})$$

$$r_{13} = -\sin(q_{11} + q_{12})$$

$$r_{31} = \sin(q_{11} + q_{12})$$

$$r_{33} = \cos(q_{11} + q_{12})$$

$$r_{22} = 1$$

$$r_{12} = r_{21} = r_{23} = r_{32} = 0$$

## B. Grasp Quality Metric

Here, a brief formulation is given to find the grasp quality while more details can be best found in [37]. The contact friction is modelled by approximating the friction cones with eight-sided pyramids having a unit length and a half angle of  $\tan^{-1} \mu_s$ , where  $\mu_s$  is the static friction coefficient as shown in Fig. 27.

Then the contact force  $f$  transfer to the object through contact is the linear combination of the vectors used to approximate the eight sides of the pyramid.

$$f = \sum_j^m \alpha_j f_j \quad (30)$$

where,  $\alpha_j > 0$ ,  $\sum_j^m \alpha_j = 1$  and number of sides of the pyramid  $m = 8$

The contact wrench can be defined as the six-dimensional vectors formed by contact forces and torques at the contact point and is given as follows.

$$\mathbf{w}_{ij} = \left( \begin{array}{c} \mathbf{f}_{ij} \\ \lambda(\mathbf{d}_i \times \mathbf{f}_{ij}) \end{array} \right) \quad (31)$$

where,  $\mathbf{f}_{ij}$  is the  $j$ -th component of the friction cone at the  $i$ -th point of contact.  $\mathbf{d}_i$  is the distance vector from torque origin to the  $i$ -th point of contact. The scalar  $\lambda$  enforces the constraint  $\|\boldsymbol{\tau}\| \leq \|f\|$ .

Now, assembling all the contact wrenches gives the convex hull or the polygon as follows.

$$W = \text{ConvexHull}\left(\bigcup_i^n \{\mathbf{w}_{i,1}, \mathbf{w}_{i,2}, \dots, \mathbf{w}_{i,m}\}\right) \quad (32)$$

The volume  $v$  of the hull gives an invariant measure of grasp quality subjected to the origin of the wrench space lies within the convex hull. This quality measure is used as a basis for the optimisation of the link dimensions.

## C. Design of Position-Based Impedance Controller

Grasping task involves a physical interaction between the finger and the object. Impedance control is preferred for a task that involves physical contact with the environment. Position-based impedance control can regulate positions and contact forces by regulating the dynamic behaviour of the system as a whole. The independent control of the two joints is not possible due to underactuated nature of the system. Here, the joints of the finger are controlled in

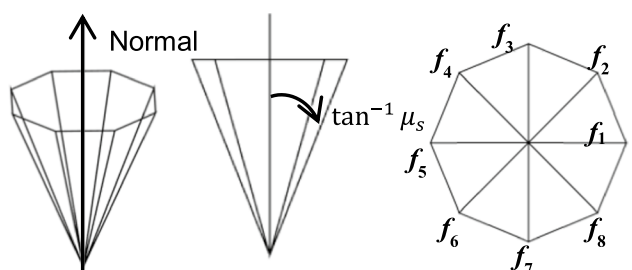
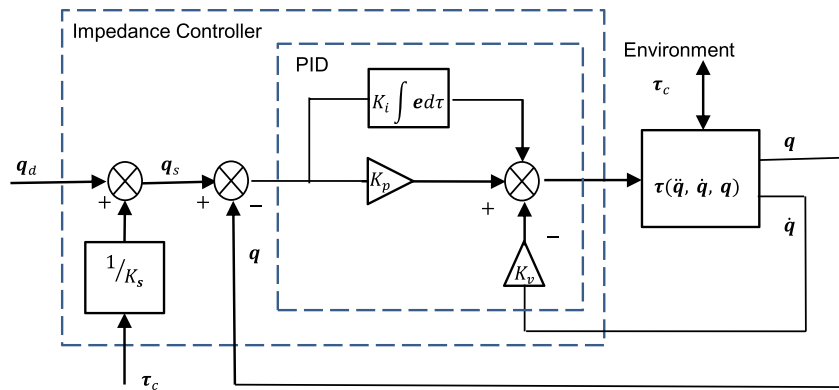


**Fig. 27** Approximation of the friction cone with an eight-sided pyramid

**Fig. 28** Block diagram of the position-based impedance controller for the gripper



joint space. The impedance controller is designed on top of a PID block as shown in Fig. 28.

Let  $q_d \in \mathbb{R}^n$  be the desired joint displacements. To achieve the desired joint trajectories and required torque for generating contact forces, the desired joint displacements are modified to a new set of joint displacement  $q_s \in \mathbb{R}^4$ . These modified displacements and actual joint displacements are used to compute displacement errors. The following PID feedback control law is used to generate the actuating torques.

$$\tau = K_p(q_s - q) - K_v\dot{q} + K_i \int (q_s - q)d\tau \quad (33)$$

where  $K_p$ ,  $K_v$ ,  $K_i$  are proportional, derivative and integral constants, respectively.

The modified joint displacements and the required joint displacements are related as follows.

$$q_s = q_d + \tau_c/K_s \quad (34)$$

where  $K_s$  is the impedance stiffness.

**Authors Contributions** All the authors have contributed to the conception and overall design of the article. The design and development of the gripper, experiments, and analysis were carried out by [SI Ansary]. The first draft of the manuscript was prepared by [SI Ansary]. The project supervision and the manuscript review and editing were performed by [Sankha Deb] and [AK Deb]. All the authors read and approved the final manuscript.

**Funding** No funding was received to assist with the preparation of this manuscript.

**Data Availability** Not applicable.

## Declarations

**Ethical Approval** Each of the authors confirms that this manuscript has not been previously published and is not currently under consideration by any other journal. Additionally, all of the authors have approved the contents of this paper and have agreed to the Journal of Intelligent and Robotic Systems submission policies.

**Consent to Participate** Not applicable.

**Consent to Publish** Not applicable.

**Competing Interests** Not applicable.

## References

- Piazza, C., Grioli, G., Catalano, M.G., Bicchi, A.: A Century of Robotic Hands. *Annu. Rev. Control Robot. Auton. Syst.* **2**(1), 1–32 (2019). <https://doi.org/10.1146/annurev-control-060117-105003>
- Birglen, L., Gosselin, C.M.: Force Analysis of Connected Differential Mechanisms: Application to Grasping. *Int. J. Robot. Res.* **25**(10), 1033–1046 (2006). <https://doi.org/10.1177/0278364906068942>
- Hirose, S.: Connected differential mechanism and its applications. In International Conference on Advanced Robotics, pp. 319–325 (1985)
- Luo, M., Mei, T., Wang, X., Yu, Y.: Grasp characteristics of an underactuated robot hand. In IEEE International Conference on Robotics and Automation, 2004. Proceedings. ICRA '04. 2004, New Orleans, LA, USA: IEEE, vol. 3, pp. 2236–2241 (2004). <https://doi.org/10.1109/ROBOT.2004.1307394>
- Rakić, M.: Multifingered robot hand with selfadaptability. *Robot. Comput.-Integr. Manuf.* **5**(2–3), 269–276 (1989). [https://doi.org/10.1016/0736-5845\(89\)90074-4](https://doi.org/10.1016/0736-5845(89)90074-4)
- Crowder, R.M.: An anthropomorphic robotic end effector. *Robot. Auton. Syst.* **7**(4), 253–268 (1991). [https://doi.org/10.1016/0921-8890\(91\)90057-R](https://doi.org/10.1016/0921-8890(91)90057-R)
- Kontoudis, G. P., Liarokapis, M., Vamvoudakis, K. G.: An Adaptive, Humanlike Robot Hand with Selective Interdigititation: Towards Robust Grasping and Dexterous, In-Hand Manipulation. In 2019 IEEE-RAS 19th International Conference on Humanoid Robots (Humanoids), Toronto, ON, Canada: IEEE, pp. 251–258 (2019). <https://doi.org/10.1109/Humanoids43949.2019.9035037>
- Zhang, Y., et al.: Design and control of the BUAA four-fingered hand. In Proceedings 2001 ICRA. IEEE International Conference on Robotics and Automation (Cat. No.01CH37164), Seoul, South Korea: IEEE, pp. 2517–2522 (2001). <https://doi.org/10.1109/ROBOT.2001.933001>
- Townsend, W.: The BarrettHand grasper – programmably flexible part handling and assembly. *Ind. Robot Int. J.* **27**(3), 181–188 (2000). <https://doi.org/10.1108/01439910010371597>
- Tamamoto, T., Koganezawa, K.: Multi-joint gripper with differential gear chain. In 2013 IEEE International Conference on

- Mechatronics and Automation, Takamatsu, Kagawa, Japan: IEEE, pp. 30–35 (2013). <https://doi.org/10.1109/ICMA.2013.6617889>
11. Lovchik, C. S., Diftler, M. A.: The Robonaut hand: a dexterous robot hand for space. In Proceedings 1999 IEEE International Conference on Robotics and Automation (Cat. No.99CH36288C), Detroit, MI, USA: IEEE, pp. 907–912 (1999). <https://doi.org/10.1109/ROBOT.1999.772420>
  12. Birglen L, Gosselin C, Laliberté T.: Underactuated robotic hands. in Springer tracts in advanced robotics, no. volume 40. Berlin: Springer (2008). <https://doi.org/10.1007/978-3-540-77459-4>
  13. Kashef, S.R., Amini, S., Akbarzadeh, A.: Robotic hand: A review on linkage-driven finger mechanisms of prosthetic hands and evaluation of the performance criteria. *Mech. Mach. Theory.* **145**, 103677 (2020). <https://doi.org/10.1016/j.mechmachtheory.2019.103677>
  14. Laliberté, T., Gosselin, C. M.: Underactuation in Space Robotic Hands. In International Symposium on Artificial Intelligence and Robotics & Automation in Space, pp. 1–8 (2001)
  15. Yang, D., et al.: An anthropomorphic robot hand developed based on underactuated mechanism and controlled by EMG signals. *J. Bionic Eng.* **6**(3), 255–263 (2009). [https://doi.org/10.1016/S1672-6529\(08\)60119-5](https://doi.org/10.1016/S1672-6529(08)60119-5)
  16. Jin, J., Zhang, W., Sun, Z., Chen, Q.: LISA Hand: Indirect self-adaptive robotic hand for robust grasping and simplicity. In 2012 IEEE International Conference on Robotics and Biomimetics (ROBIO), Guangzhou, China: IEEE, pp. 2393–2398 (2012). <https://doi.org/10.1109/ROBIO.2012.6491328>
  17. Cheng, M., Jiang, L., Ni, F., Fan, S., Liu, Y., Liu, H.: Design of a highly integrated underactuated finger towards prosthetic hand. In 2017 IEEE International Conference on Advanced Intelligent Mechatronics (AIM), Munich, Germany: IEEE, pp. 1035–1040 (2017). <https://doi.org/10.1109/AIM.2017.8014155>
  18. Li, X., Huang, Q., Chen, X., Yu, Z., Zhu, J., Han, J.: A novel under-actuated bionic hand and its grasping stability analysis. *Adv. Mech. Eng.* **9**(2), 168781401668885 (2017). <https://doi.org/10.1177/1687814016688859>
  19. Hirose, S., Umetani, Y.: The development of soft gripper for the versatile robot hand. *Mech. Mach. Theory.* **13**(3), 351–359 (1978). [https://doi.org/10.1016/0094-114X\(78\)90059-9](https://doi.org/10.1016/0094-114X(78)90059-9)
  20. Kaneko, M., Higashimori, M., Takenaka, R., Namiki, A., Ishikawa, M.: The 100 G capturing robot - too fast to see. *IEEE/ASME Trans. Mechatron.* **8**(1), 37–44 (2003). <https://doi.org/10.1109/TMECH.2003.809137>
  21. Massa, B., Roccella, S., Carrozza, M. C., Dario P.: Design and development of an underactuated prosthetic hand. In Proceedings 2002 IEEE International Conference on Robotics and Automation (Cat. No.02CH37292), Washington, DC, USA: IEEE, pp. 3374–3379 (2002). <https://doi.org/10.1109/ROBOT.2002.1014232>
  22. Carrozza, M.C., et al.: The SPRING Hand: Development of a Self-Adaptive Prosthesis for Restoring Natural Grasping. *Auton. Robots.* **16**(2), 125–141 (2004). <https://doi.org/10.1023/B:AURO.0000016863.48502.98>
  23. Gosselin, C., Pelletier, F., Laliberte T.: An anthropomorphic underactuated robotic hand with 15 dofs and a single actuator. In 2008 IEEE International Conference on Robotics and Automation, Pasadena, CA, USA: IEEE, pp. 749–754 (2008). <https://doi.org/10.1109/ROBOT.2008.4543295>
  24. Ciocarlie, M., et al.: The Velo gripper: A versatile single-actuator design for enveloping, parallel and fingertip grasps. *Int. J. Robot. Res.* **33**(5), 753–767 (2014). <https://doi.org/10.1177/0278364913519148>
  25. Sainul I. A., Deb, S., Deb, A. K.: A three finger tendon driven robotic hand design and its kinematics model, in CAD/CAM, robotics and factories of the future, D. K. Mandal and C. S. Syan, Eds., in Lecture Notes in Mechanical Engineering. New Delhi: Springer India, pp. 313–321 (2016). [https://doi.org/10.1007/978-81-322-2740-3\\_30](https://doi.org/10.1007/978-81-322-2740-3_30)
  26. Ozawa, R., Tahara, K.: Grasp and dexterous manipulation of multi-fingered robotic hands: a review from a control view point. *Adv. Robot.* **31**(19–20), 1030–1050 (2017). <https://doi.org/10.1080/01691864.2017.1365011>
  27. Stojanovic, V., Nedic, N.: Joint state and parameter robust estimation of stochastic nonlinear systems. *Int. J. Robust Nonlinear Control.* **26**(14), 3058–3074 (2016). <https://doi.org/10.1002/rnc.3490>
  28. Birglen, L., Gosselin, C.M.: Geometric Design of Three-Phalanx Underactuated Fingers. *J. Mech. Des.* **128**(2), 356–364 (2006). <https://doi.org/10.1115/1.2159029>
  29. Ozawa, R., Hashirii, K., Yoshimura, Y., Moriya, M., Kobayashi, H.: Design and control of a three-fingered tendon-driven robotic hand with active and passive tendons. *Auton. Robots.* **36**(1–2), 67–78 (2014). <https://doi.org/10.1007/s10514-013-9362-z>
  30. Ferrari, C., Canny, J.: Planning optimal grasps. In Proceedings 1992 IEEE International Conference on Robotics and Automation, Nice, France: IEEE Comput. Soc. Press, pp. 2290–2295 (1992). <https://doi.org/10.1109/ROBOT.1992.219918>
  31. Ciocarlie, M., Allen, P.: Data-driven optimization for underactuated robotic hands. In 2010 IEEE International Conference on Robotics and Automation, Anchorage, AK: IEEE, pp. 1292–1299 (2010). <https://doi.org/10.1109/ROBOT.2010.5509793>
  32. Kirkpatrick, S., Gelatt, C.D., Vecchi, M.P.: Optimization by Simulated Annealing. *Science.* **220**(4598), 671–680 (1983). <https://doi.org/10.1126/science.220.4598.671>
  33. Coleman, T.F., Li, Y.: A Reflective Newton Method for Minimizing a Quadratic Function Subject to Bounds on Some of the Variables. *SIAM J. Optim.* **6**(4), 1040–1058 (1996). <https://doi.org/10.1137/S1052623494240456>
  34. Shilane, P., Min, P., Kazhdan, M., Funkhouser, T.: The princeton shape benchmark. In Proceedings Shape Modeling Applications, 2004., Genova, Italy: IEEE, pp. 167–388 (2004). <https://doi.org/10.1109/SMI.2004.1314504>
  35. Kasper, A., Xue, Z., Dillmann, R.: The KIT object models database: An object model database for object recognition, localization and manipulation in service robotics. *Int. J. Robot. Res.* **31**(8), 927–934 (2012). <https://doi.org/10.1177/0278364912445831>
  36. Ansary, S.I., Deb, S., Deb, A.K.: A novel object slicing-based grasp planner for unknown 3D objects. *Intell. Serv. Robot.* **15**(1), 9–26 (2022). <https://doi.org/10.1007/s11370-021-00397-0>
  37. Miller, A. T., Allen, P. K.: Examples of 3D grasp quality computations. In Proceedings 1999 IEEE International Conference on Robotics and Automation (Cat. No.99CH36288C), Detroit, MI, USA: IEEE, pp. 1240–1246 (1999). <https://doi.org/10.1109/ROBOT.1999.772531>

**Publisher's Note** Springer Nature remains neutral with regard to jurisdictional claims in published maps and institutional affiliations.

Springer Nature or its licensor (e.g. a society or other partner) holds exclusive rights to this article under a publishing agreement with the author(s) or other rightsholder(s); author self-archiving of the accepted manuscript version of this article is solely governed by the terms of such publishing agreement and applicable law.

**Sainul Islam Ansary** received his B.E. (Hons.) degree in Electronics and Communication Engineering from the University Institute of Technology, Burdwan University and M. Tech in Robotics from Indian Institute of Information Technology Allahabad, India in 2012 and 2014, respectively. He obtained his PhD in Robotics from Indian Institute of Technology Kharagpur, India in 2023. He worked as a Research Engineer in an industrial project at CoE-AMT, IIT Kharagpur in 2021. He is currently a Postdoctoral Researcher at Poznan University of Technology, Poland. His research interests include robot learning and control, robotic hands, grasping and manipulation, and robot vision.

**Sankha Deb** obtained his Ph.D. in Industrial Engineering from Ecole Polytechnique Montreal, Canada and Master's degree in Manufacturing Process Engineering from IIT Kharagpur. He served as Assistant Professor in the Centre for Soft Computing Research at ISI Kolkata and also in the Department of Mechanical Engineering at IIT Guwahati. He was invited as a Visiting Professor in University of Montreal, Canada in 2008 and 2009. He also served the Industry for a year. Presently he is an Associate Professor in the Department of Mechanical Engineering at IIT Kharagpur. His research interests are in the areas of Automation and Robotics, Manufacturing Processes, Computer Integrated Manufacturing, and Artificial Intelligence and Soft Computing applications in manufacturing. He coauthored a book on Robotics Technology and Flexible Automation.

**Prof. Alok Kanti Deb** received the B.E. (Hons) degree in electrical engineering from the Bengal Engineering College, Calcutta University, Howrah, India, and the M.Tech. (Control Engg. and Instrumentation)

and Ph.D degrees in electrical engineering from IIT Delhi, Delhi., India in 1994, 1999 and 2006 respectively. He is currently a Professor with the Department of Electrical Engineering, IIT Kharagpur, Kharagpur, India. His research interests include control systems, computational intelligence and automotive diagnostics. He has published several papers in international journals and international conferences, 1 book chapter and co-authored the book, "Industrial Instrumentation, Control and Automation", published by Jaico, Mumbai, 2013. He is the holder of the patent, "State Estimation, Diagnosis and Control Using Equivalent Time Sampling" (US Patent No. – 8,751,097 B2, dt, June 10, 2014). He regularly reviews papers from several journals and conferences. He was Vice Chair (Educational Activities), IEEE India Council-2015 and Chair, IEEE Kharagpur section 2016.

## Terms and Conditions

Springer Nature journal content, brought to you courtesy of Springer Nature Customer Service Center GmbH (“Springer Nature”). Springer Nature supports a reasonable amount of sharing of research papers by authors, subscribers and authorised users (“Users”), for small-scale personal, non-commercial use provided that all copyright, trade and service marks and other proprietary notices are maintained. By accessing, sharing, receiving or otherwise using the Springer Nature journal content you agree to these terms of use (“Terms”). For these purposes, Springer Nature considers academic use (by researchers and students) to be non-commercial.

These Terms are supplementary and will apply in addition to any applicable website terms and conditions, a relevant site licence or a personal subscription. These Terms will prevail over any conflict or ambiguity with regards to the relevant terms, a site licence or a personal subscription (to the extent of the conflict or ambiguity only). For Creative Commons-licensed articles, the terms of the Creative Commons license used will apply.

We collect and use personal data to provide access to the Springer Nature journal content. We may also use these personal data internally within ResearchGate and Springer Nature and as agreed share it, in an anonymised way, for purposes of tracking, analysis and reporting. We will not otherwise disclose your personal data outside the ResearchGate or the Springer Nature group of companies unless we have your permission as detailed in the Privacy Policy.

While Users may use the Springer Nature journal content for small scale, personal non-commercial use, it is important to note that Users may not:

1. use such content for the purpose of providing other users with access on a regular or large scale basis or as a means to circumvent access control;
2. use such content where to do so would be considered a criminal or statutory offence in any jurisdiction, or gives rise to civil liability, or is otherwise unlawful;
3. falsely or misleadingly imply or suggest endorsement, approval , sponsorship, or association unless explicitly agreed to by Springer Nature in writing;
4. use bots or other automated methods to access the content or redirect messages
5. override any security feature or exclusionary protocol; or
6. share the content in order to create substitute for Springer Nature products or services or a systematic database of Springer Nature journal content.

In line with the restriction against commercial use, Springer Nature does not permit the creation of a product or service that creates revenue, royalties, rent or income from our content or its inclusion as part of a paid for service or for other commercial gain. Springer Nature journal content cannot be used for inter-library loans and librarians may not upload Springer Nature journal content on a large scale into their, or any other, institutional repository.

These terms of use are reviewed regularly and may be amended at any time. Springer Nature is not obligated to publish any information or content on this website and may remove it or features or functionality at our sole discretion, at any time with or without notice. Springer Nature may revoke this licence to you at any time and remove access to any copies of the Springer Nature journal content which have been saved.

To the fullest extent permitted by law, Springer Nature makes no warranties, representations or guarantees to Users, either express or implied with respect to the Springer nature journal content and all parties disclaim and waive any implied warranties or warranties imposed by law, including merchantability or fitness for any particular purpose.

Please note that these rights do not automatically extend to content, data or other material published by Springer Nature that may be licensed from third parties.

If you would like to use or distribute our Springer Nature journal content to a wider audience or on a regular basis or in any other manner not expressly permitted by these Terms, please contact Springer Nature at

[onlineservice@springernature.com](mailto:onlineservice@springernature.com)